Electronic Supplementary Material (ESI) for Nanoscale.

Supplementary Information for Critical Peeling of Tethered Nanoribbons

Andrea Silva,[1,2,*] Erio Tosatti,[2,3,1] and Andrea Vanossi[1,2]

[1] *CNR-IOM, Consiglio Nazionale delle Ricerche - Istituto Officina dei Materiali, c/o SISSA Via Bonomea 265, 34136 Trieste, Italy*

[2] *International School for Advanced Studies (SISSA), Via Bonomea 265, 34136 Trieste, Italy.*

[3] *The Abdus Salam International Centre for Theoretical Physics (ICTP), Strada Costiera 11, 34151 Trieste, Italy*

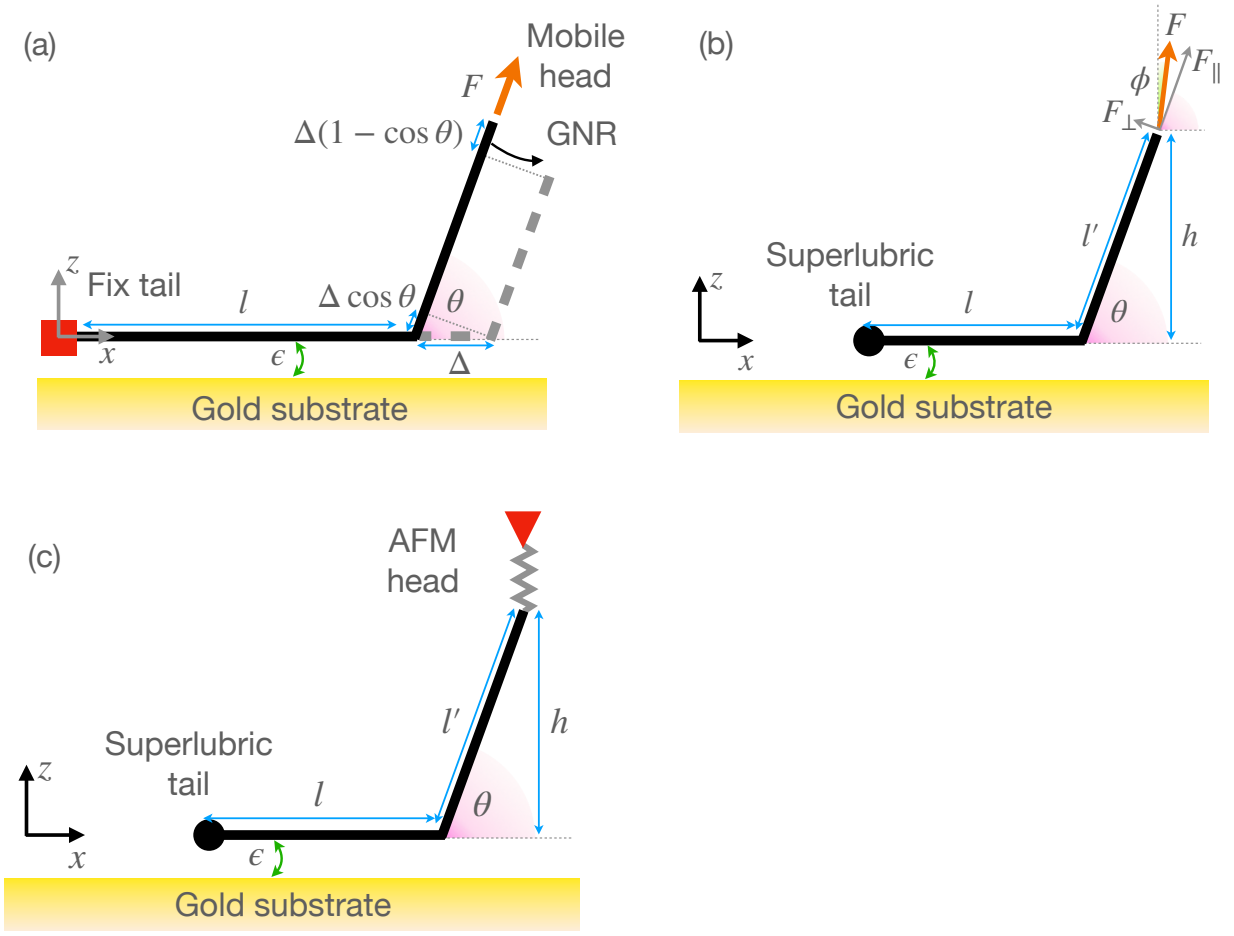

FIG. 1. (a) Kendall setup. The tail is fix while the head is free to move in xz. The ribbon is shown as a solid black line. Dashed gray segments represent a previous configuration of the ribbon. The application point of the force changes as the peeling proceeds. This change is the projection of the peeled front advancement Δ on the direction of the force. (b) Setup between Kendall and AFM: the ribbon peels at an angle θ under a constant-force at an angle ϕ acting at fixed coordinate x during the lifting. The tail can slide without friction while the head is fixed at the starting x coordinate. The application point of the force changes in z only. (c) AFM-like setup. The AFM is moving on a timescale larger than the relaxation time of the GNR. Thus, it is considered at a fixed height h and exerting the necessary force to maintain the GNR in this position, i.e. the force is can vary.

* ansilva@sissa.it

I. CLASSIC MODELS

Consider a GNR of length L as sketched in fig. 1. The GNR adheres to a smooth metal surface, such as Au(111), with a strength ϵ, in units of energy over length. The head is attached via a spring A to an AFM tip, whose end at height h above the surface is being lifted. We shall consider the head spring to be infinitely stiff $A \to \infty$, so that the head of the of GNR follows the AFM tip without delay.

A. Classic Kendall model

In the Kendall [1] configuration the head is lifted at constant force F and the application points can move horizontally and vertically. On the other side, the tail is fix. The lifted part of the GNR is extensible, with Young modulus Y. Following Kendall assumptions, we shall not consider the bending rigidity of the GNR, resulting in a sharp profile at the detachment point. The energy of the system as a function of the attached fraction l and the detached part δ is composed of four terms: the adhesive energy, the work done on the system by the external force, the extension of the ribbon and the shift in the force application point

$$E(l) = -\epsilon l \ - \int_0^{L-l} \vec{F} \cdot \vec{\Delta} dx \ + \frac{\tilde{K}}{2}\delta^2 \ + F\delta, \tag{1}$$

where Δ is the peeling segment, see fig. 1a. The work done by the applied force can be written as $\int_0^{L-l} \vec{F} \cdot \vec{\Delta} dx = F(L-l)(1-\cos\theta)$, see fig. 1a. From classical elasticity theory [1], the effective spring constant of the GNR is $\tilde{K} = Y/(L-l)$, being $(L-l)$ the rest length of the detached part and the elastic displacement due to F is $\delta = F(L-l)/Y$. Thus eq. (1) becomes

$$E(l) = -\epsilon l \ - F(L-l)(1-\cos\theta) \ - \frac{1}{2}\frac{F^2(L-l)}{Y}. \tag{2}$$

The equilibrium configuration satisfies $\frac{\partial E}{\partial l} = 0$, i.e.

$$-\epsilon + F(1-\cos\theta) + \frac{1}{2}\frac{F^2}{Y} = 0, \tag{3}$$

which is equivalent to equation 2 in Ref. [1]. In the limit of inextensible GNR, $\lim Y \to \infty$, equation 5 in Ref. [1] is recovered

$$F = \frac{\epsilon}{1-\cos\theta} \tag{4}$$

or $\cos\theta = 1 - \frac{\epsilon}{F}$. The peeling proceeds at constant angle and constant force, with the peeling front moving towards the tail.

B. AFM-Kendall Model

Let us now consider a setup closer to AFM experiments. As sketched in fig. 1b, the AFM tip, considerably more massive than the GNR, operates at fix x, y coordinates and the GNR slides over the substrate without resistance: the tail can advance while the point of application of the force is fixed in the x direction. In AFM experiments the applied force F is thus always vertical. For the sake of linking the Kendall setup to the AFM setup, consider a fictitious system in which an angle ϕ is present between the force F and the z axis while the GNR peels at an angle θ, as shown in fig. 1b.

The energy in this case is

$$E(l) = -\epsilon l \ - F(L-l)\sin\theta\cos\phi - \frac{1}{2}F\sin(\phi+\theta)^2\frac{(L-l)}{Y}.$$

At equilibrium

$$-\epsilon \ + F\sin\theta\cos\phi \ + \frac{1}{2}\frac{(F\sin(\phi+\theta)^2}{Y} = 0, \tag{5}$$

which is the counterpart of eq. (3) in this geometry. For $\phi = \pi/2 - \theta$, i.e. F parallel to the lifted fraction as in Kendall, the condition eq. (5)

$$-\epsilon \ + F(\sin\theta)^2 \ + \frac{1}{2}\frac{F^2}{Y} = 0. \tag{6}$$

For $\phi = 0$, i.e. F vertical, the condition eq. (5)

$$-\epsilon \ + (F\sin\theta) \ + \frac{1}{2}\frac{(F\sin\theta)^2}{Y} = 0. \tag{7}$$

In the limit of inextensible GNR ($Y \to \infty$), both eqs. (6) and (7) become

$$F = \epsilon/\sin(\theta). \tag{8}$$

Thus, the functional form of the peeling evolution in this setup is different from the original Kendall system but the underlying physical principle is unchanged. Note that for $\theta = \pi/2$ the solutions in eqs. (3), (6) and (7) are equivalent. The force F is minimal and the configurations become the same: vertical peeling.

C. Adiabatic Peeling

In AFM experiments, the tip is lifted extremely slowly ($v \approx \mu$m/s), on a timescale orders of magnitude larger than the relaxation time of the GNR. The peeling is *adiabatic*, with the

GNR relaxing to the mechanically stable configuration at each height reached by the AFM tip. Thus, in this experimental setup is more realistic to work at constant height h rather than constant force F. The assumption is that the ideal constraint point will applying the minimum force necessary to keep the head of the GNR at the desired height h.

Let us focus on inextensible GNR, i.e. Young modulus $Y \to \infty$, and neglect bending rigidity. Thus the length L of the GNR is preserved during the peeling. In this framework, the state of ribbon can be expressed as a function of the peeling angle, which is now free to vary, as sketched in fig. 1c. This setup represent the conjugate, constant-height version of the Kendall model.

The energy is a function of θ and depends parametrically on the lifting height h:

$$E(\theta; h) = -\epsilon l = -\epsilon(L - \frac{h}{\sin\theta}). \tag{9}$$

At equilibrium

$$\frac{\partial E(\theta; h)}{\partial \theta} = -\epsilon \frac{h}{\sin^2\theta}\cos\theta = 0, \tag{10}$$

which has the only solution $\theta = \pi/2$. This is a Gigli-like solution [2], without bending rigidity: the tail advances until the detachment front is below the tip and the peeling proceeds at a right angle. During the peeling the force $F = \partial E/\partial h$ is constant $[F]_{\pi/2} = \epsilon$. This behaviour is in agreement with Kendall's results in eq. (8): the minimum value of the peeling force is found at vertical peeling.

II. ANALYTIC MODEL ADDITIONAL DETAILS

A. Energy economy for $L = 30\,\mathrm{nm}$

Figure 2 reports the total energy, the adhesion energy, the tether energy and the derivative of the force with respect to h for the $L = 30\,\mathrm{nm}$ case discussed in the main text.

B. Infinite length limit

The configuration and energy economy of a modelled ribbon of length $L = 1 \times 10^6\,\text{Å}$ is reported in fig. 3. All points at a finite Q reach the steady state.

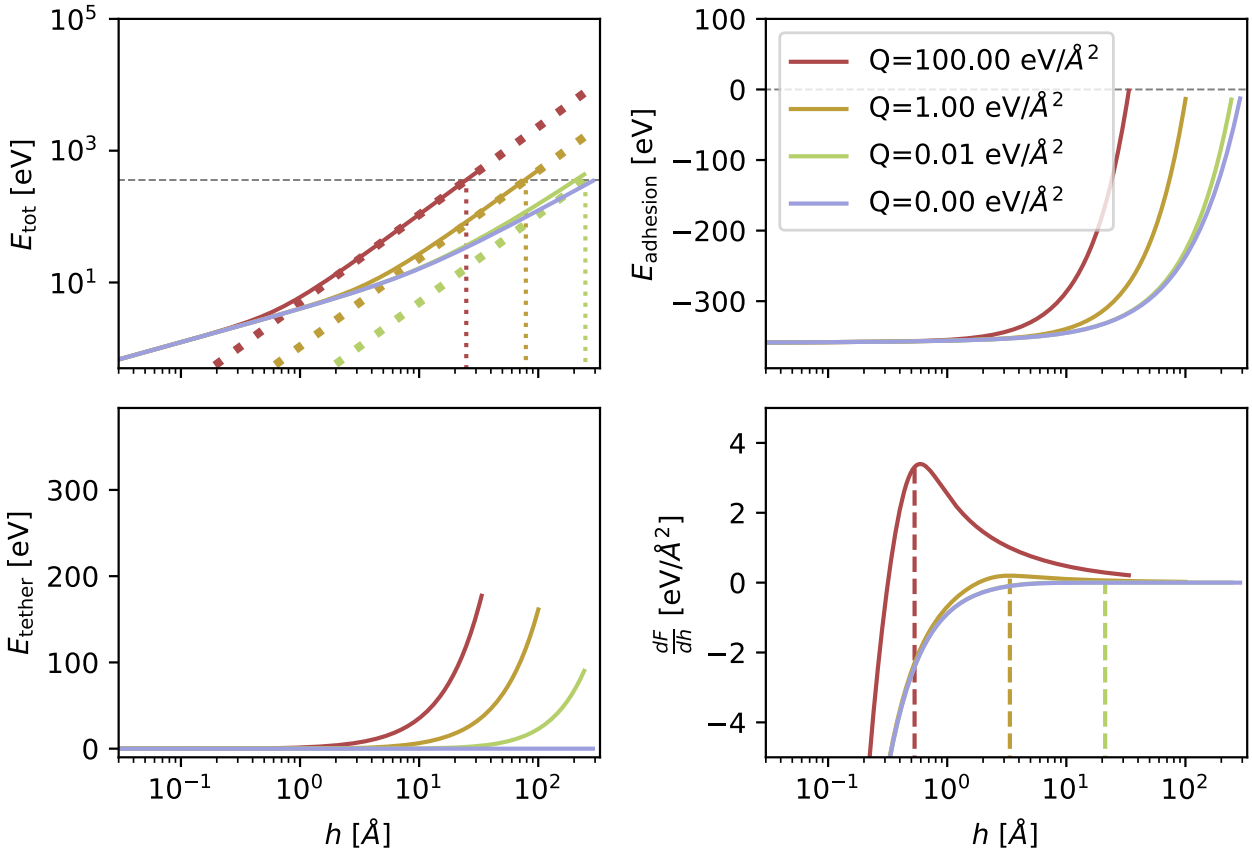

FIG. 2. (a) Total energy, (b) the adhesion energy, (c) the tether energy and (d) the derivative of the force with respect to h. See the main text for definitions.

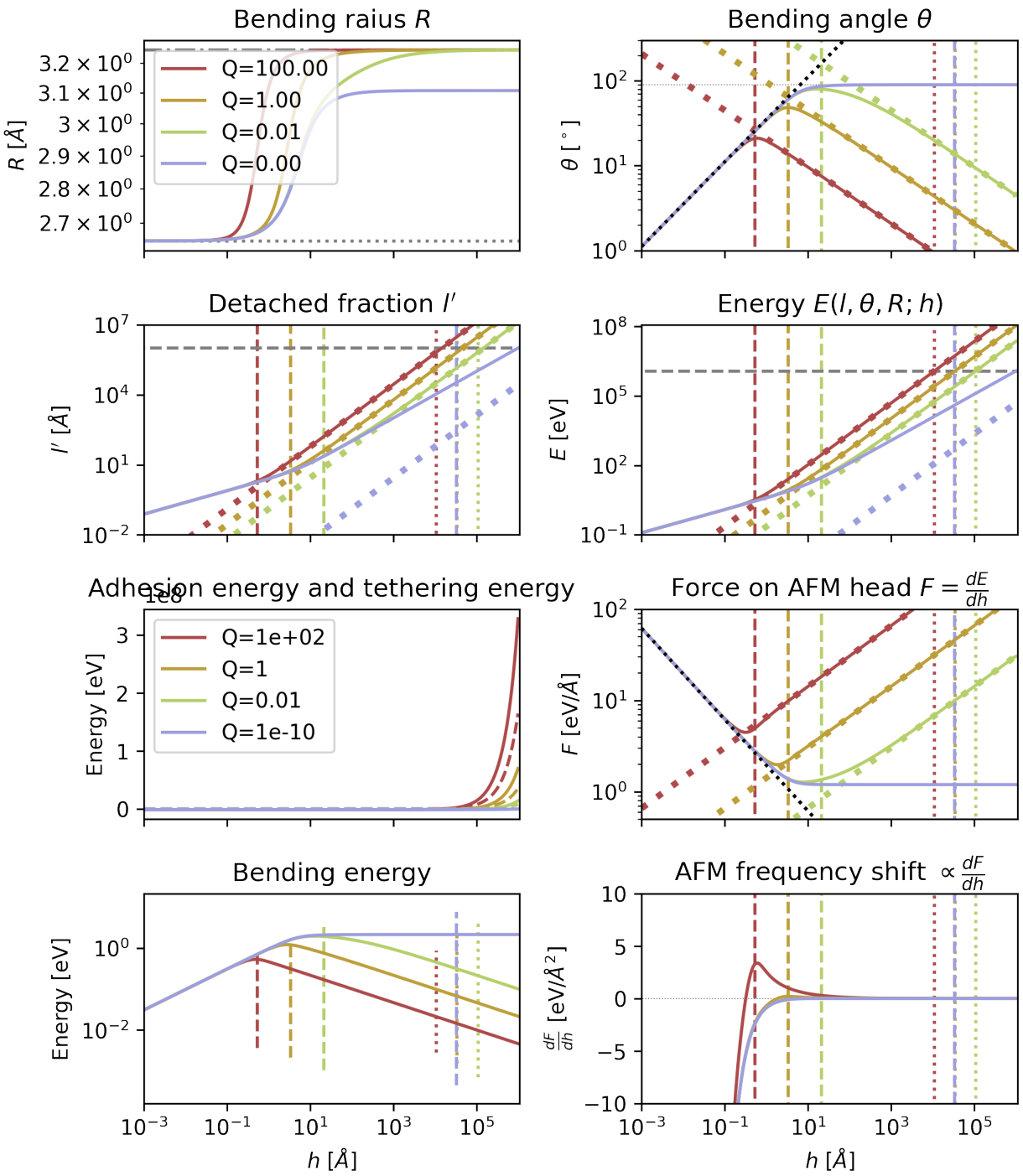

FIG. 3. Configuration, energy contributions and force of the system in the model for $L = 1 \times 10^6$ Å.

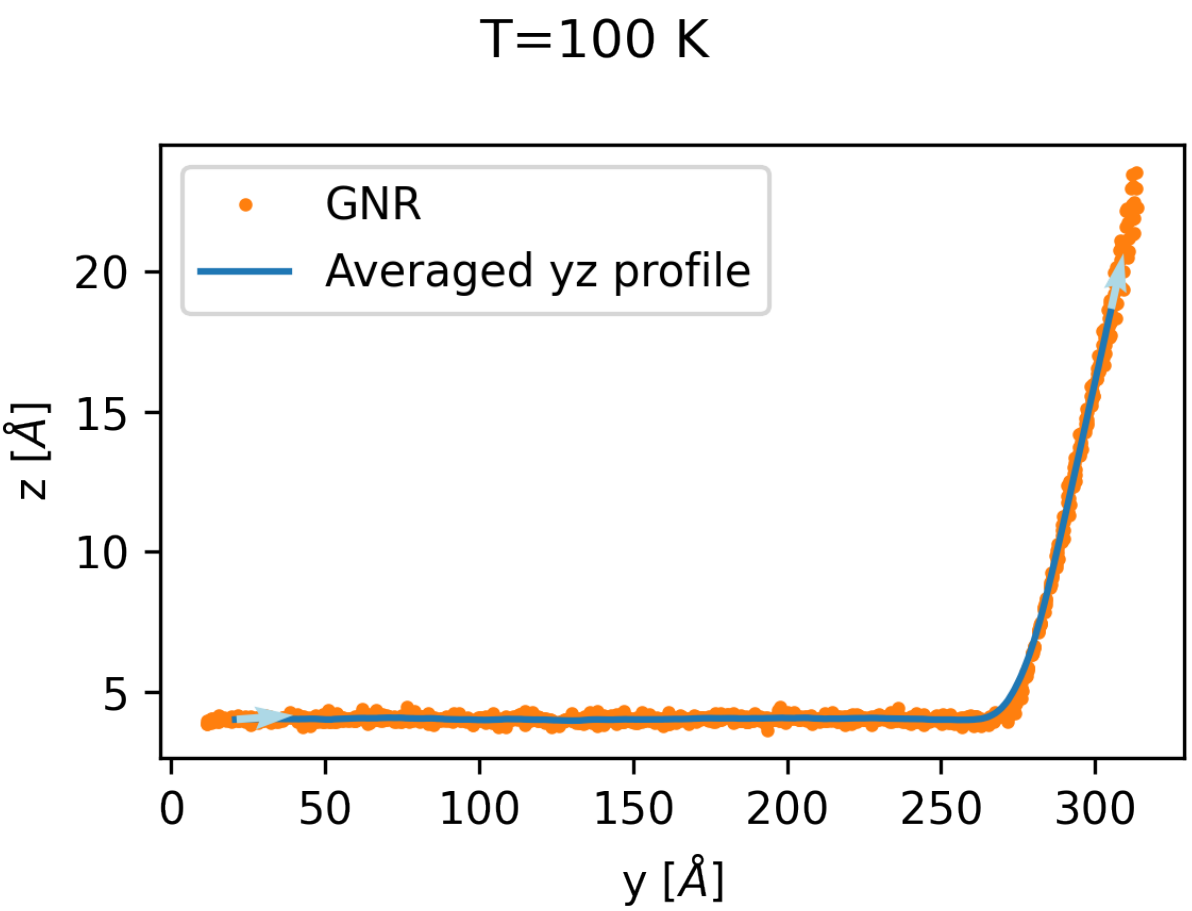

FIG. 4. Smoothing GNR lateral profile at finite temperature $T = 100\,\mathrm{K}$. Orange points are C atoms. The solid line represent the profile used to compute the peeling angle. The profile is obtained from a running average over the y, z coordinates.

III. BENDING ANGLE ESTIMATION

Figure 4 shows how the peeling angle in MD simulations is computed. First the GNR profile (orange points in fig. 4) is smoothed by a running average (window $n = 80$ atoms) along the x and y directions (blue solid line in fig. 4). The tangent to this line is estimated by compute the gradient numerically. The angle between the first and last segments of the smoothed profile (arrows in fig. 4) is used to estimated the peeling angle.

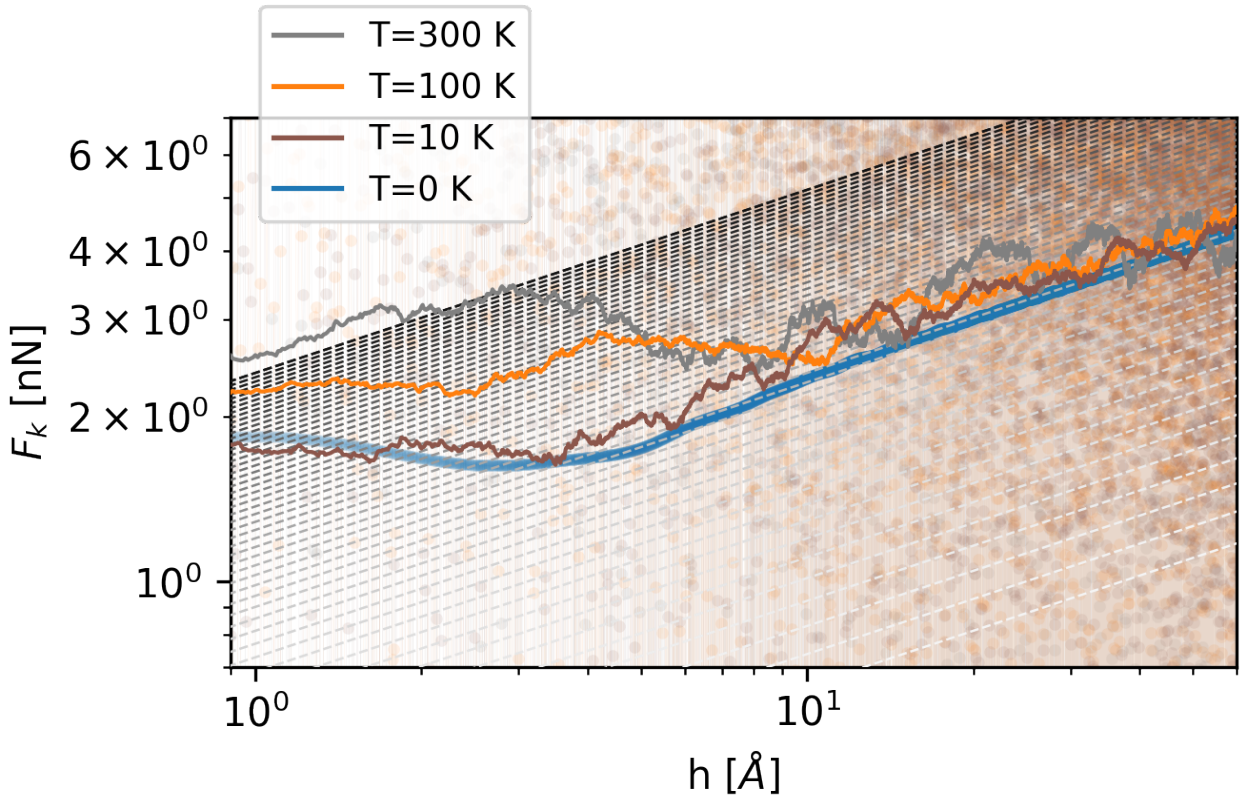

FIG. 5. Force on the AFM tip in finite temperature simulations for $Q = 0.5\,\mathrm{eV/Å^2}$. Points are recorded values during the MD simulations, solid lines are a running average of width $N = 500$ time-steps. Dashed lines in grayscale mark the $F \propto h^{1/3}$ behaviour as a guide to the eye.

IV. FINITE TEMPERATURE

To understand the effect of temperature on the system, we focus on an intermediate tethering $Q = 0.5\,\mathrm{eV/Å^2}$ and simulate the peeling at increasing temperatures. Figure 5 reports the peeling force for temperatures from 0 to 300 K. The detached fraction of the GNR behaves as a defective guitar string that keeps detuning as it vibrates. The extremely soft flexural mode of graphene deforms the GNR at almost no cost and, as the tip rises, large oscillation appear in the lifted fraction. These oscillations intermittently change side in the competition between the adhesive energy and the tip force to move the position of the peeling front, see Supplementary Movie 2. When the adhesion and thermal fluctuation work together, the peeling front moves closer to the x coordinate of the tip; hence the

adsorbed fraction increases and the peeling force suddenly increases. When fluctuations and the vertical tip pulling are allies, the peeling front retreats towards the tail, reducing the peeling force. In the latter, if the fluctuation is large enough, it can even compress the tip spring, resulting in a negative force, a behaviour not possible at zero temperature. The soft flexural mode of the GNR adds a substantial noise to the force trace (semi-transparent dots in fig. 5) that clouds the signal even after a running average over 500 configurations (solid lines in fig. 5). The zero-temperature scaling behaviour is not clearly detected here for curves above 10 K.

A clearer signal is obtained from the peeling angle θ, as reported in the Conclusions in main text.

V. SUPPLEMENTARY MOVIE 1

Peeling at different Q: blue $Q = 0\,\mathrm{eV/\AA^2}$, red $Q = 0.001\,\mathrm{eV/\AA^2}$, gray $Q = 0.146\,\mathrm{eV/\AA^2}$, yellow $Q = 0.5\,\mathrm{eV/\AA^2}$, green $Q = 50\,\mathrm{eV/\AA^2}$.

VI. SUPPLEMENTARY MOVIE 2

Intrinsic oscillations of the GNR at $Q = 0.5\,\mathrm{eV/\AA^2}$. The oscillations are created by lifting the center of the detached part of $\delta = 10\,\mathrm{\AA}$ and letting the system evolve in NVE setup.

[1] K. Kendall, Thin-film peeling-the elastic term, Journal of Physics D: Applied Physics **8**, 1449 (1975).

[2] L. Gigli, A. Vanossi, and E. Tosatti, Modeling nanoribbon peeling, Nanoscale **11**, 17396 (2019).